Wang et al. Journal of Palaeogeography (2020) 9:9
https://doi.org/10.1186/s42501-020-00058-w

Journal of Palaeogeography

ORIGINAL ARTICLE

Open Access

Sedimentary characteristics of microbialites influenced by volcanic eruption: a case study from the Lower Cretaceous Shipu Group in Zhejiang Province, East China

Xiao-Fang Wang[1,2,3,4], Xiu-Cheng Tan[1,2,3*], Shao-Nan Zhang[1,2], An-Jiang Shen[3,4], Chang Li[3,4], Guang Hu[1,2,3], Xin Wang[3,4], Zi-Liao Chen[3,4], Li-Yin Pan[3,4], Jie Zhang[3,4] and Wei Chen[3,4]

Abstract

This study describes a sequence of microbialites and volcanics of the Lower Cretaceous Shipu Group, an example of microbialites influenced by volcanic activity. It is located at Shipu town in eastern Zhejiang Province on the coast of southeastern China. Based on macroscopic outcrop observations, microscopic examination of thin sections, electron probe microanalysis (EPMA), field emission scanning electron microscopy (FESEM) imaging analysis, and energy dispersive X-ray spectrometry (EDS) analysis, nine microbialite–tuffite assemblages have been recognized in the section. Their thickness increased gradually upwards as volcanism decreased. There are ooids, bioclastic grains, intraclasts and tuffaceous grains in the grain shoal with local dolomitization. Above the grain shoal, microbial reefs develop either individually or conjoining with adjacent ones, and consist of stromatolites and serpulid tubes with common recrystallization. Tubes of serpulids are calcified and the tube wall is micrite. The tube and intertube parts are filled by sparry calcite. Colonial serpulids are surrounded by microbes to form stromatolites. Black layers of stromatolites contain many calcite crystals with fan-shaped growth pattern and preserved organic matter. Microbes are so well preserved in crystal lattices that the original microstructure of the microbes can be clearly observed by FESEM imaging analysis. Microbial reefs develop at a local high point near or above fair-weather wave-base where waves removed fine volcanic ashes. Interreef deposits are coarse tuffite due to physical differentiation. Volcanic activity could provide rich nutrition for microbes, but too much fine volcanic ash inhibits microbial growth. As a result, a moderate supply of volcanic ash favors the development of microbialites.

Keywords: Microbialite, Stromatolites, Tuffite, Lower Cretaceous, Shipu Group

1 Introduction

With the recent discovery of hydrocarbons in microbial carbonate reservoirs, such as the Gulf of Mexico in America (Mancini et al. 2008), Santos Basin in Brazil (Rezende and Pope 2015), and the Sichuan Basin in China (Li et al. 2013; Che et al. 2019), microbialite research has become a hotspot. In the geological record, microbialites may develop both in marine (Burne and Moore 1987; Riding 1991, 2000; Kershaw et al. 2007, 2012; Delfino et al. 2012; Bahniuk et al. 2015; Tang et al. 2017) and lacustrine facies (Lei et al. 2012; Tang et al. 2012; Della Porta 2015; Zhang et al. 2018). However, they are rarely found in strata influenced by volcanic eruptions. This paper describes the sedimentary characteristics of microbialites affected by volcanic activity. The Shipu microbialite-bearing section, commonly termed "the Shipu limestone", is located at Shipu town,

* Correspondence: tanxiucheng70@163.com
[1]State Key Laboratory of Oil and Gas Geology and Exploitation, Southwest Petroleum University, Chengdu 610500, Sichuan Province, China
[2]School of Geoscience and Technology, Southwest Petroleum University, Chengdu 610500, Sichuan Province, China
Full list of author information is available at the end of the article

Xiangshan county in eastern Zhejiang Province on the coast of southeastern China along the coastal lowlands of the western Pacific Ocean (Fig. 1). These well-preserved microbialites have not previously been investigated. This study provides an opportunity to investigate the sedimentary characteristics of microbialites influenced by volcanic activity. Based on macroscopic observation of the outcrop, microscopic examination of thin sections, together with EPMA, FESEM and EDS, assemblage features of the microbialites and tuffite have been elucidated. The effects of volcanic activity are also made clear.

2 Geological setting

Since the Early Cretaceous, the study area experienced two basin-building stages. The first occurred at approximately 145–100 Ma ago (Early Cretaceous) and was characterized by volcanic faulted-depressions (Jahn 1974; John et al. 1990; Zhou et al. 2006). The second occurred at approximately 100–70 Ma ago (Late Cretaceous–Paleogene) and is characterized by red-colored sedimentary rocks. Corresponding to this two-stage basin development, the Lower Cretaceous is composed of rhyolite, lava,

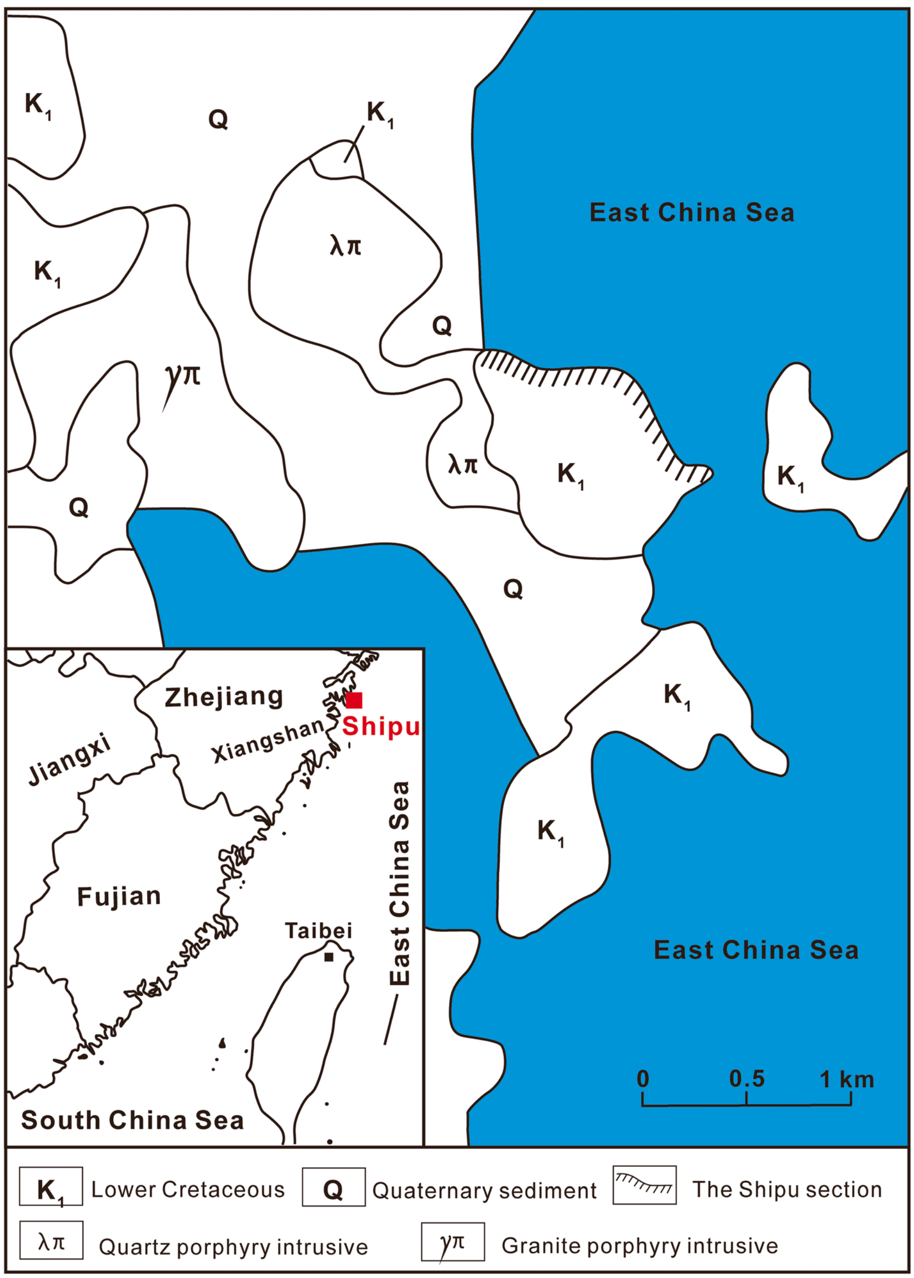

Fig. 1 Location map of the Shipu section in Xiangshan county, eastern Zhejiang Province, China

volcanic agglomerate, volcanic breccia, sedimentary volcaniclastic rocks, tuffite and some carbonates (Fig. 2). The Upper Cretaceous consists mainly of red siltstone, mudstone, and intercalated basalt. The Paleogene comprises mostly grey to purple coarse-grained clastic rocks, siltstone, mudstone and intercalated gypsum, and oil-bearing shale. The Neogene is composed of brown to yellow siltstones and is present locally (Hu et al. 2012a).

During the Early Cretaceous, seawater transgressed into the area that is now coastal southeastern China and limestones were deposited in coastal

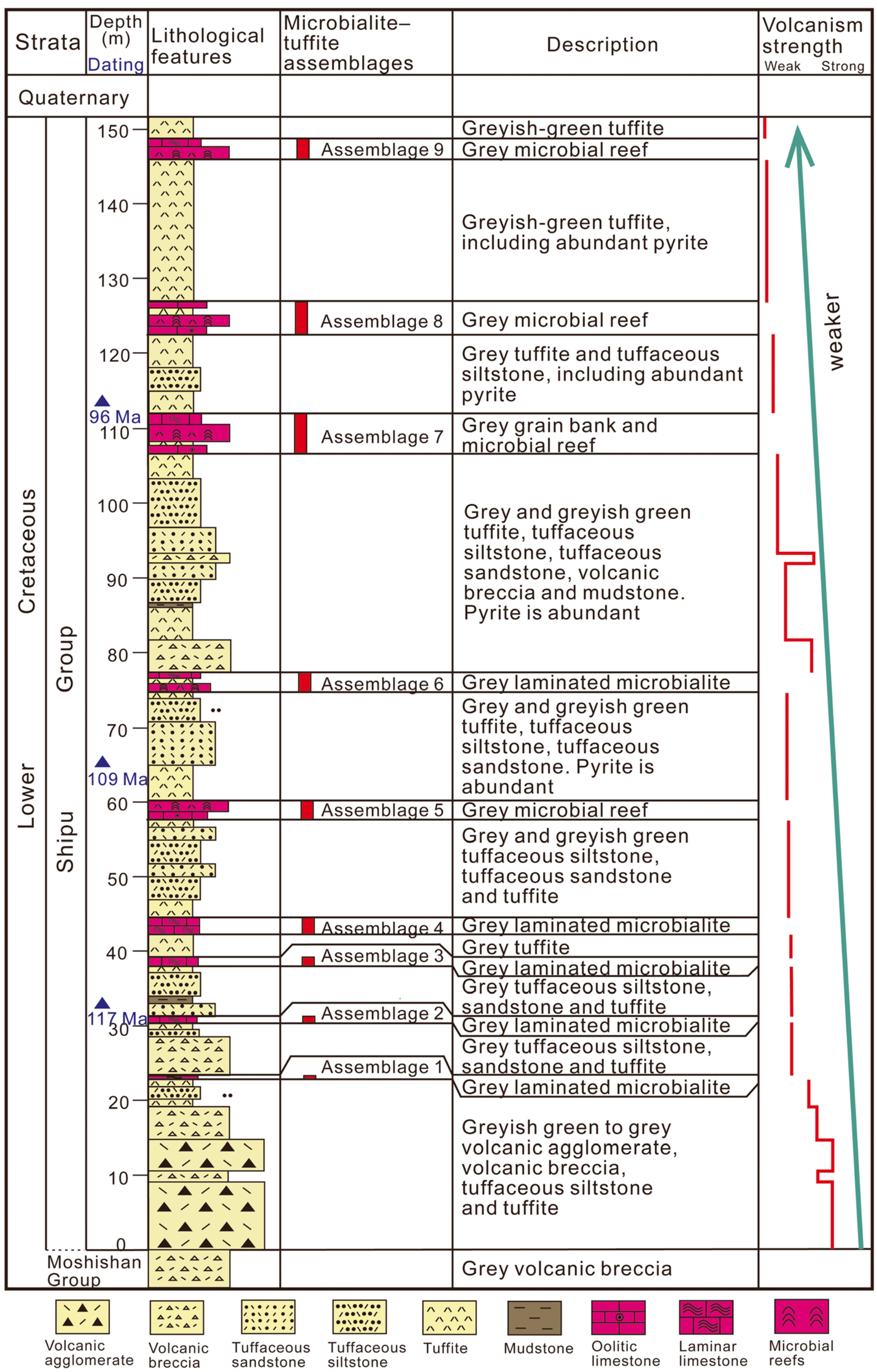

Fig. 2 Generalized stratigraphic column of the Shipu section showing nine microbialite-tuffite assemblages

environments ranging from tidal flats to shallow marine (Xu and Zheng 1989; Xu 1991, 1992; Xie et al. 2010; Hu et al. 2012a, b; Xu et al. 2018).

In Shipu town, Xiangshan county, Zhejiang Province, the base of the section has faulted contact with volcanic breccia and ignimbrites of the Lower Cretaceous Moshishan Group, and the top is covered by Quaternary sediments (Fig. 2; Hu et al. 2012a).

3 Stratigraphy

As shown in Fig. 2, the total thickness of Shipu section is 150 m. The lower part of the section (0–30 m) consists mainly of volcanic agglomerate, volcanic breccia and tuffaceous sandstone. The middle part (31–105 m) contains mainly silicified tuffaceous sandstones, silicified tuffaceous siltstones, rhyolite, lava, silicified tuffites and microbialites. In contrast, the upper part (106–150 m) is composed mainly of

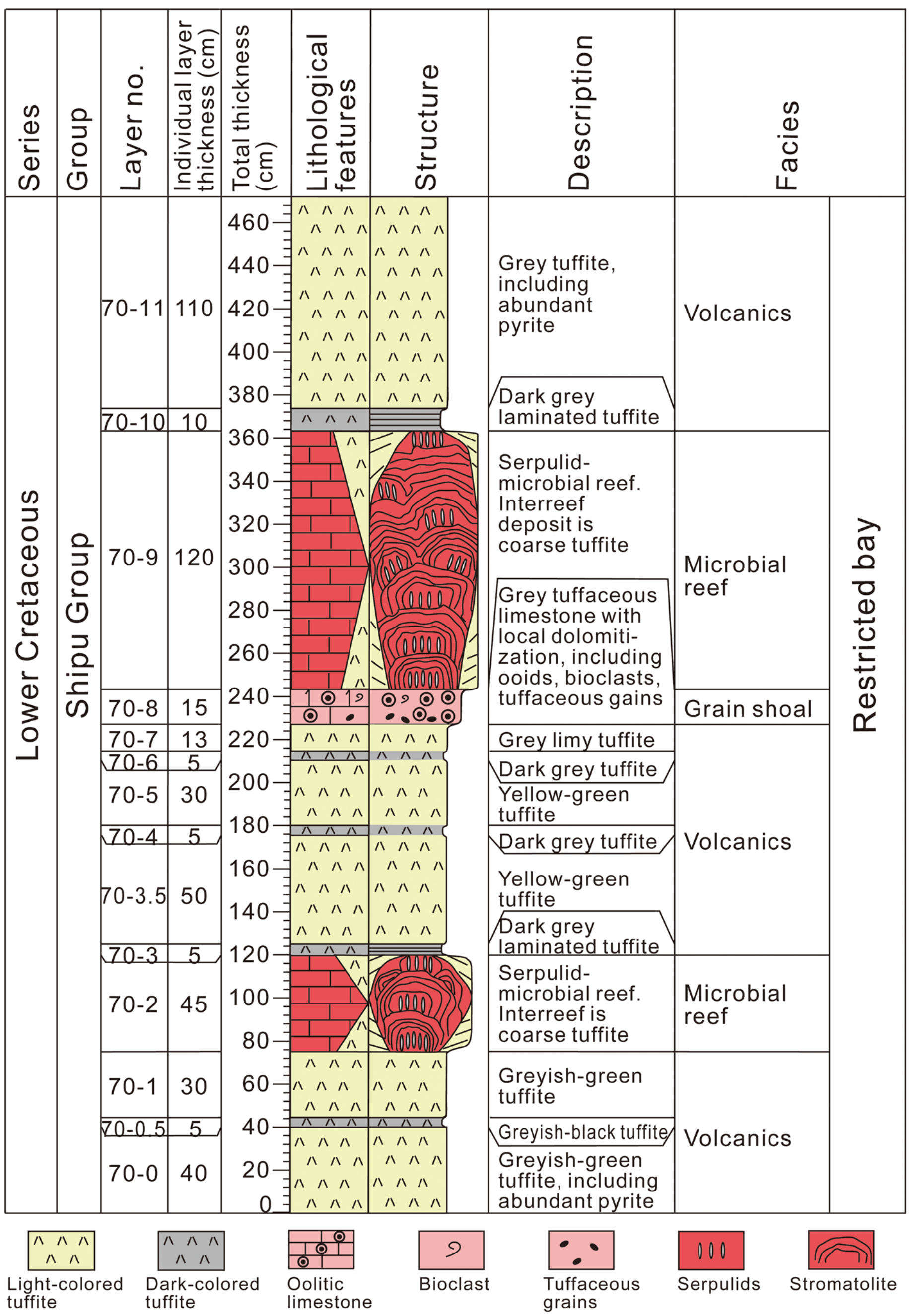

Fig. 3 Generalized stratigraphic column of the microbialite-tuffite assemblage 8 of the Shipu section

silicified tuffites, microbialites and silicified tuffaceous siltstones. There are nine microbialite–tuffite assemblages in the section, and their thickness increases gradually upwards, as volcanism strength gradually decreases (Fig. 2).

4 Methods

In the Shipu section of the Lower Cretaceous Shipu Group, nine microbialite–tuffite assemblages were observed and measured. One hundred fifty-nine samples were examined in polished hand specimens and in corresponding thin-sections that were partially stained with Alizarin red S and potassium ferricyanide (Dickson 1966) to distinguish calcite and dolomite. Thin-sections were compared with their corresponding hand specimens in order to relate the macroscopic features to the accretion process, as interpreted by petrographic study. Polished slabs of microbialites were prepared for macrostructure observation. Petrologic thin sections of microbialites were made to examine fabrics.

Thirty-eight representative thin-sections of the various lithologies were examined by EPMA and EDS to identify the minerals, owing to complexity of these mixed carbonate and volcanic rocks.

In order to observe possible microbial signatures within stromatolites, freshly broken and polished chips of laminated structure were prepared for FESEM. These samples were cleaned by diluted water and then etched with 0.5% chloride acid for 3–5 s, followed by a second rinse by diluted water and ethyl alcohol. Some samples for FESEM analysis were polished with wide beam argon ion polishing instrument. Some were entirely coated with platinum for surface texture analysis and EDS analysis. These analyses were conducted in the Key Laboratory of Carbonate Reservoirs, CNPC, China.

5 Features of microbialite–tuffite assemblage

Because the lithology of the Shipu section is very complicated, when the strength of volcanic activity was very strong, microbialites could not develop. In order to elucidate features of the microbialites and the effects of volcanics associated with them, we chose the microbialite–tuffite assemblage 8 (see Fig. 2) to illustrate them in detail (Fig. 3). From bottom to top, Layers 70-0 to 70-1 are

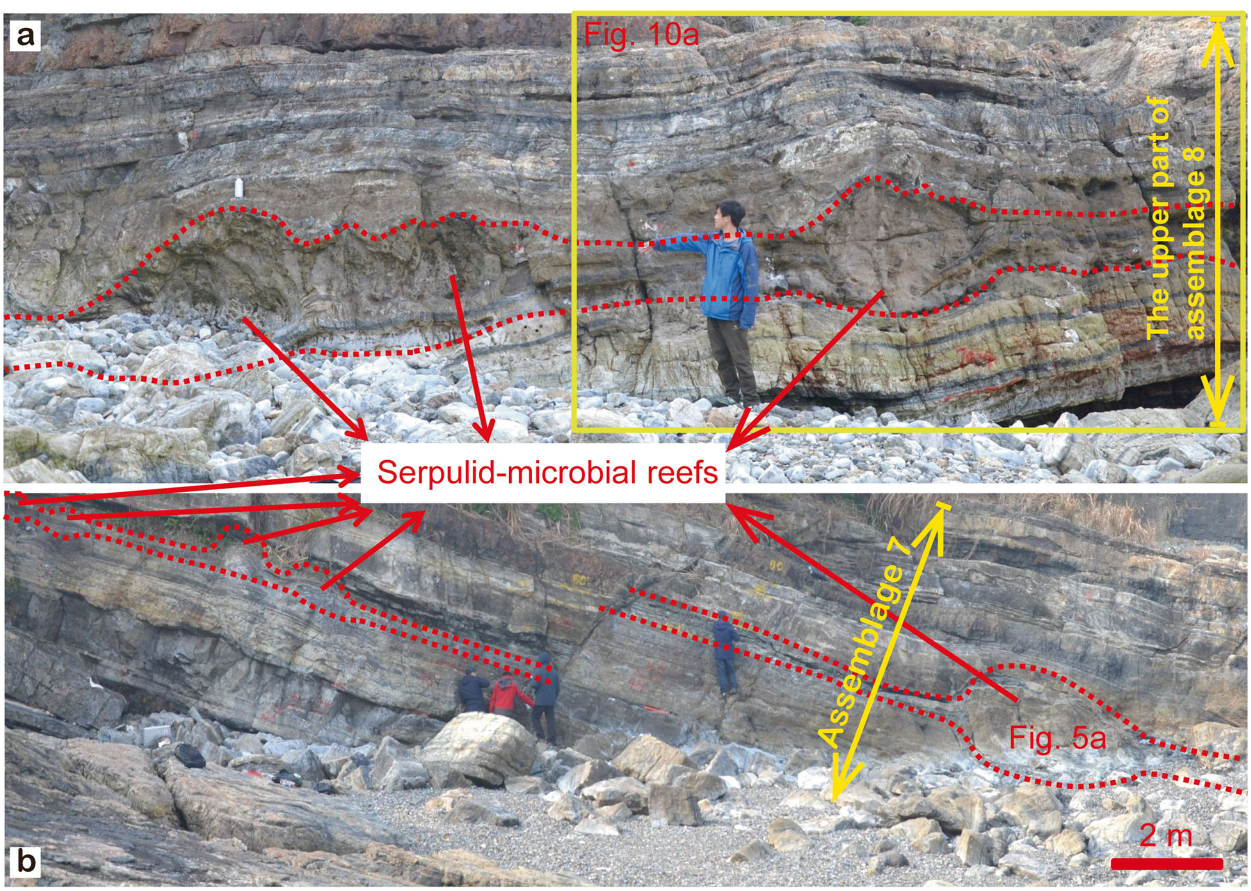

Fig. 4 Field photo showing macro-structures of serpulid-microbial reefs in the upper part of assemblage 8 (**a**) and assemblage 7 (**b**) of the Shipu section. The person in a is 1.7 m tall for scale

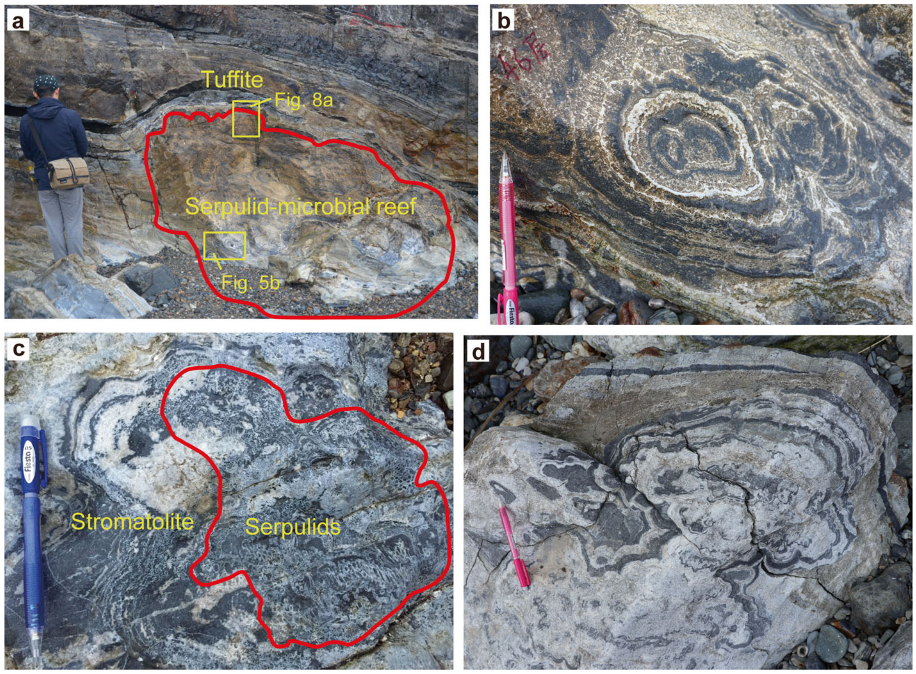

Fig. 5 a Field photograph showing the largest reef in the assemblage 7 which contains stromatolites and serpulids. Above the reef is laminated fine tuffite; **b** Domal stromatolites showing that bright layers and dark layers are interlayered; **c** Colonial serpulid tubes are surrounded by microbes to form a small reef; **d** Microbial reef without serpulid tubes. Person in **a** is 1.7 m tall; Pens in **b**–**d** are 14 cm long for scale

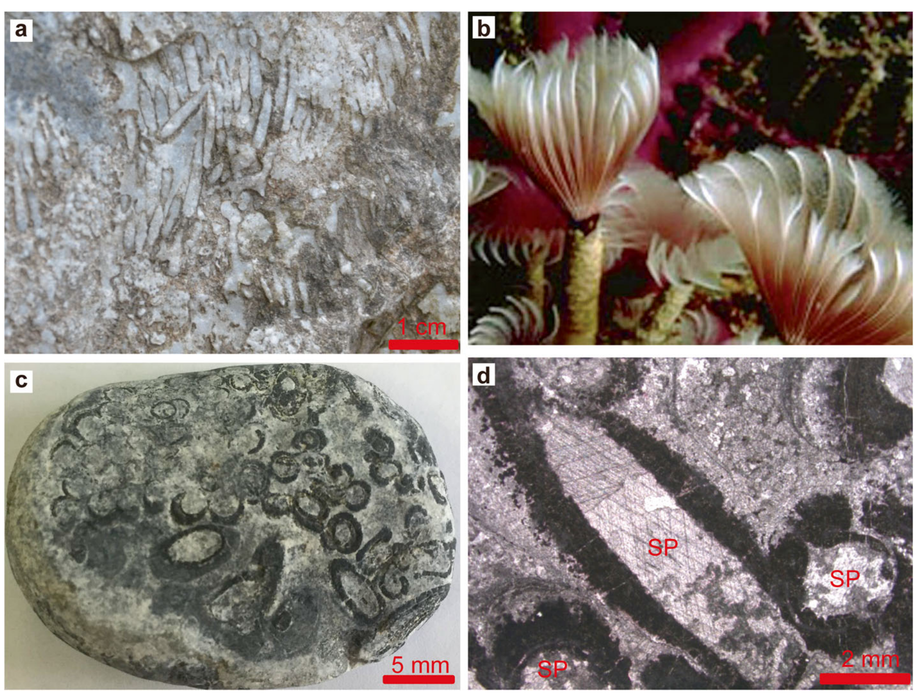

Fig. 6 a Field meso-photo showing colonial serpulid tubes; **b** Modern serpulids: their tubes are calcareous but their tentacles cannot be calcified and preserved after they die (photograph from the internet); **c** A hand specimen showing colonial serpulid tubes. Every dark circle is the micritic wall of a serpulid tube; **d** Photomicrograph showing micritic walls of serpulid (SP) tubes. The inner parts of the serpulid tubes have been infilled by sparry calcite. 1.25×, plane-polarized light greyish-green tuffite with greyish-black tuffite interlayers. Layer 70-2 is serpulid-microbial reef with interreef deposit of coarse tuffite. Above the reef, Layer 70-3 is a 5-cm-thick tuffite which is dark grey and laminated. Layers 70-3.5 to 70-6 are yellow-green tuffite with dark grey tuffite interlayers. Layer 70-7 is grey limy tuffite. Layer 70-8 is a grain shoal deposit. The lower part of shoal is grey tuffaceous limestone, whereas the upper part is dolomitic grainstone including ooids, bioclasts and intraclasts. Above the grain shoal, Layer 70-9 is another serpulid-microbial reef layer and the interreef is coarse tuffite. Above the reefs, Layer 70-10, a 10-cm-thick laminated tuffite inhibited further reef growth. There are therefore three main lithologies in this assemblage of microbialites and tuffites: (1) carbonates; (2) tuffite; (3) mixed lithology.

5.1 Microbialites

5.1.1 Stromatolites (limestone)

As shown in Fig. 4, stromatolites developed in the reef where microbes and serpulids built the framework together. Serpulid-microbial reefs coalesced with adjacent ones or individually. Among them, the largest is 2.0 m wide and 1.7 m high (Figs. 4 and 5a). Colonial serpulids are surrounded by microbes which trapped and bound grains to form reef framework (Fig. 5c). Stromatolites

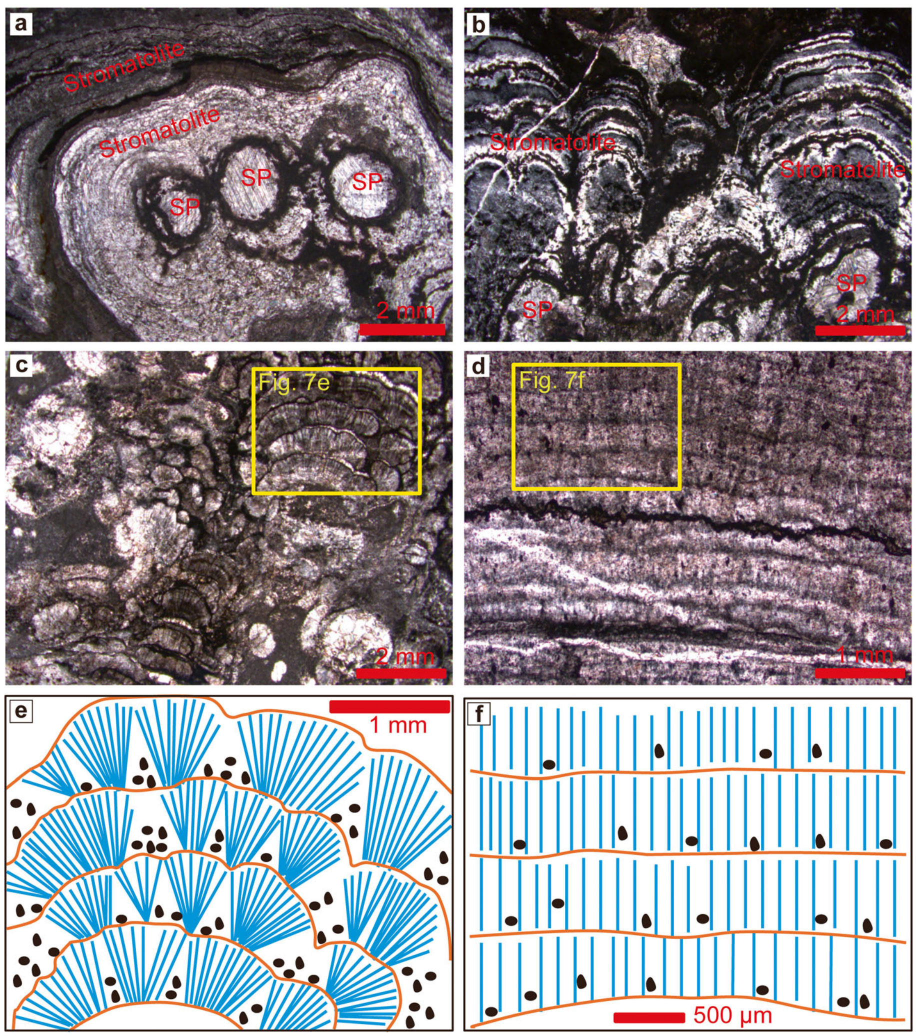

Fig. 7 **a** Photomicrograph showing stromatolites and serpulid (SP) tubes. Walls of serpulid tubes remain micrite but the tube interiors and some adjacent laminae have been infilled by, or recrystallized to, sparry calcite. The outermost peripheral laminae are still micrite which look much darker. 1.25×, plane-polarized light; **b** Microbes grew surrounding the tube walls and accreted to form columnar stromatolites. 1.25×, plane-polarized light; **c**, **e** Fan-shaped stromatolites accreted through the growth of colonies of filamentous microbes (probably cyanobacteria) and with the early and pervasive precipitation of carbonate in the EPS sheaths of their filaments. Grains supplied on the stromatolite surface were not trapped and bound in the microbial EPS, but only deposited between the filament fans (Suarez-Gonzalez et al. 2019). Orange lines represent thin micritic crust. 1.25×, plane-polarized light; **d**, **f** Flat-shaped stromatolites accreted through the growth of other microbes (blue lines) and grains were trapped and bound in the uncalcified EPS. Thin micritic crusts (orange lines) separating successive laminae formed during interruptions in accretion. 2.5×, plane-polarized light

show distinct macroscopic lamination (Fig. 5b–d) formed by dark and light laminae. Serpulids commonly live in groups (Fig. 6). Their calcareous tubes can be preserved (Fig. 6c–d) but their tentacles cannot be calcified and are not preserved after their death. The walls of their calcareous tubes remained micritic and are filled by sparry calcite (Fig. 6c–d). Microbes, such as cyanobacteria or others, surrounded the colonial serpulids and grew to form stromatolites by calcification and trapping and binding grains (Fig. 7). In the Shipu section, two kinds of accretion processes generated stromatolites: (1) Fan-shaped stromatolites accreted through the growth of colonies of filamentous microbes (probably cyanobacteria) and the early and pervasive precipitation of carbonate in the extracellular polymeric substances (EPS) sheaths of their filaments (Figs. 7c, e, 8b, c and 11c). Grains supplied on the stromatolite surface were not trapped and bound in the microbial EPS, but only deposited between the filament fans (Suarez-Gonzalez et al. 2019). (2) Flat-shaped stromatolites accreted through the growth of other microbes and grains were trapped and bound in the uncalcified EPS (Fig. 7d, f). Thin micritic crusts (orange lines) separate successive laminae and formed during interruption in accretion.

In order to search for possible microbial signatures within stromatolites (Li et al. 2017), freshly broken and polished chips (using a wide beam argon ion polishing instrument) from a darker layer in the stromatolites were prepared for FESEM imaging analysis. These samples were coated with platinum for surface texture analysis and EDS analysis. As shown in Fig. 8, a sample from the top of a reef was chosen to search for the microbes which may occur in the darker laminae (red rectangle, Fig. 8a). Under plane-polarized light, photomicrographs show stromatolites with well-preserved fan-shaped growth pattern (Fig. 8b, c). A FESEM image of a freshly broken chip from a darker layer shows calcite crystals,

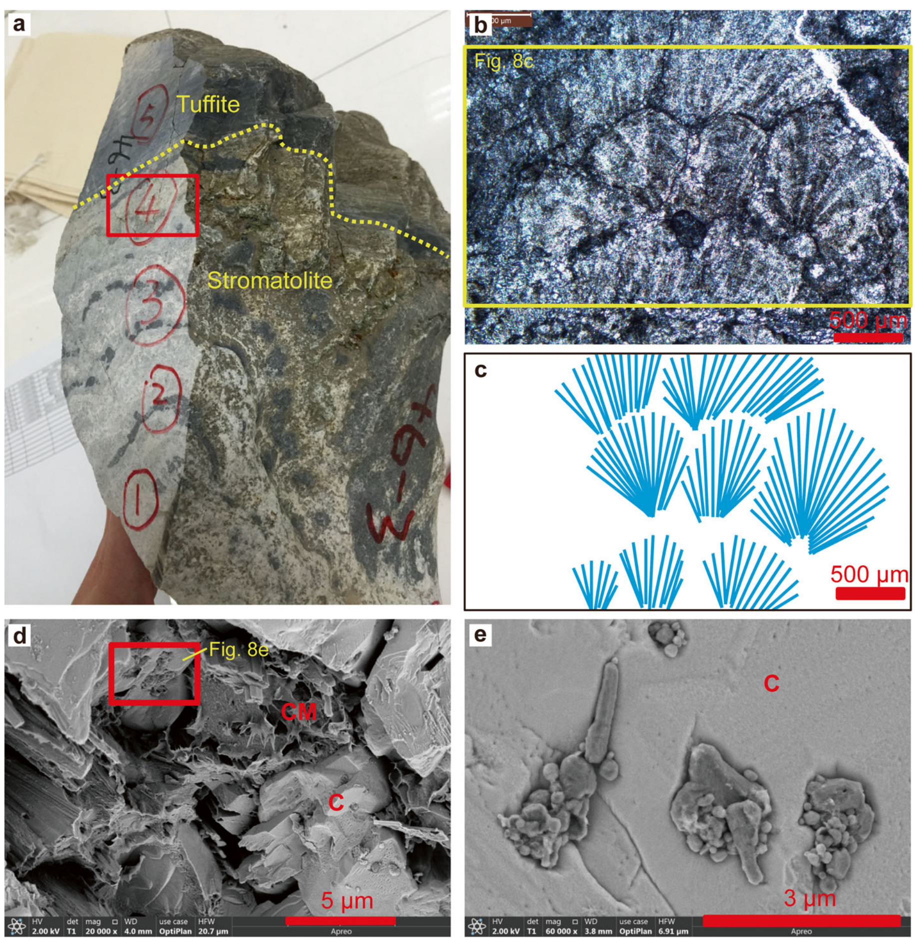

Fig. 8 a Meso-photo of a hand specimen from the top of a reef showing that the upper part is tuffite, and the lower part is stromatolite (limestone) which contains bright layers and dark layers. Finger of 1.5 cm wide in the lower left corner for scale; **b** Photomicrograph of stromatolite (limestone) from the dark layer (red rectangle in **a**) showing its accretion in a fan-shaped growth pattern (see **c**). 5×, plane-polarized light; **d** FESEM image of a freshly broken chip from a darker layer showing calcite (C) crystals, clay minerals (CM) and suspected microbes (red rectangle); **e** Suspected microbes are highlighted in details; the host is a calcite (C) crystal clay minerals and suspected microbes (Fig. 8d). Many microbial remains can be seen in FESEM photomicrographs which are displayed in a relatively darker color (Figs. 8e and 9a). In calcite crystals, some microbes are preserved so well that the cells can be clearly seen in FESEM photomicrographs of polished samples (Fig. 9d–f). EDS analysis shows that the carbon element content is high, up to 71.1 wt% (Fig. 9c), and that the host is a calcite crystal (Fig. 9b).

5.1.2 Oolitic limestone with bioclasts and intraclasts

Oolitic limestone occurs in the upper part of Layer 70-8 (Figs. 3 and 10), which is 15–20 cm thick below the serpulid-microbial reef. Layer 70-8 is a grain bank that developed in a high-energy zone near or above fair-weather wave-base (FWWB) and is mainly composed of oolitic limestone, including bioclasts and intraclasts (Fig. 10c–f), with local dolomitization (Fig. 10d). A whole fossil gastropod can be seen in Fig. 10e.

5.2 Tuffites

Tuffite is a volcanic ash deposit, which implies that the study area was relatively far away from the volcanic crater. Tuffite occurs above and below the microbialites, and is also deposited in interreef environments.

5.2.1 Laminated fine tuffite

Laminated fine tuffite that developed above the reefs is 5–10 cm thick (Fig. 3). A sample (Figs. 10a and 11a) from the interface between reef and tuffite shows that the upper part of it is laminated fine tuffite (Fig. 11b) and that the

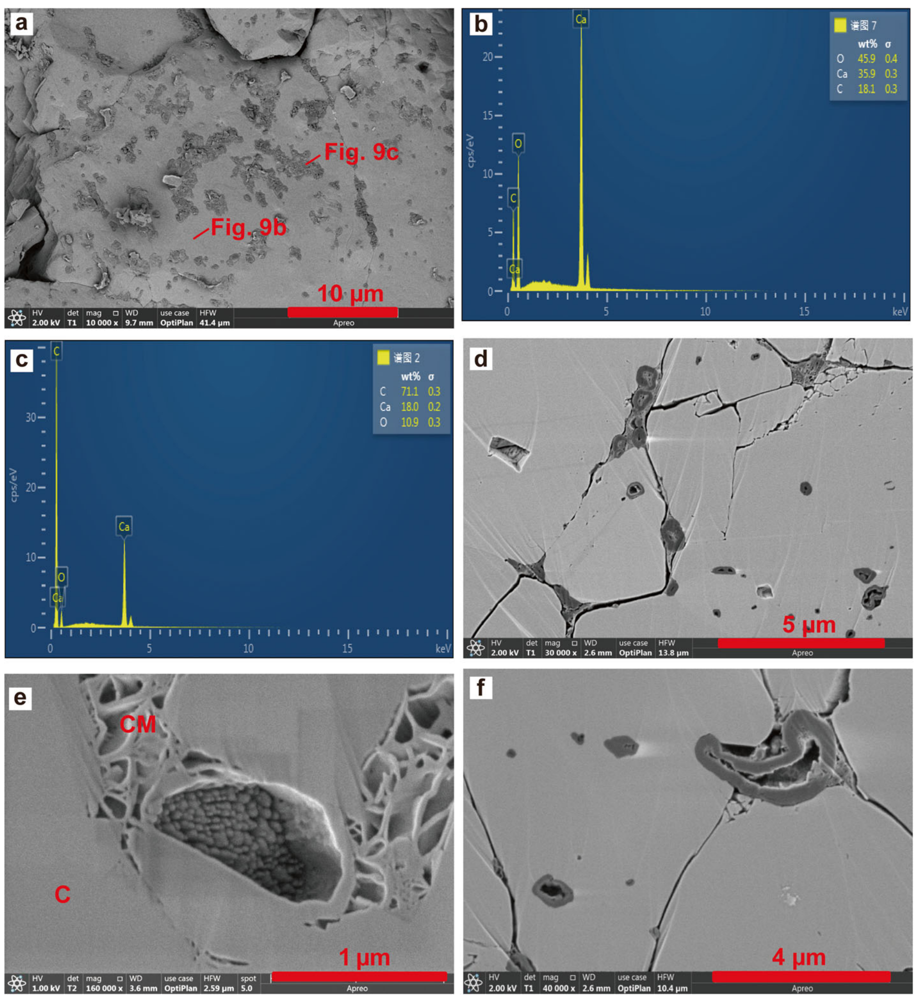

Fig. 9 **a** A FESEM image of a freshly broken chip from a darker layer of stromatolite showing many suspected microbes in dark color above the surface of calcite crystals. EDS analysis shows that the light-colored host consists of calcite crystals (**b**) whereas the dark-colored matter is suspected microbes (organic matter) (**c**); **d** A FESEM image of a polished chip showing that there is much organic matter (in dark color) remaining in intercrystalline spaces of calcite; **e** A FESEM image of a polished chip showing calcite crystal (C), clay mineral (CM) and suspected microbes; **f** A FESEM image of a polished chip showing residual organic matter in intercrystalline spaces which looks like the cells of microbes (in dark color)

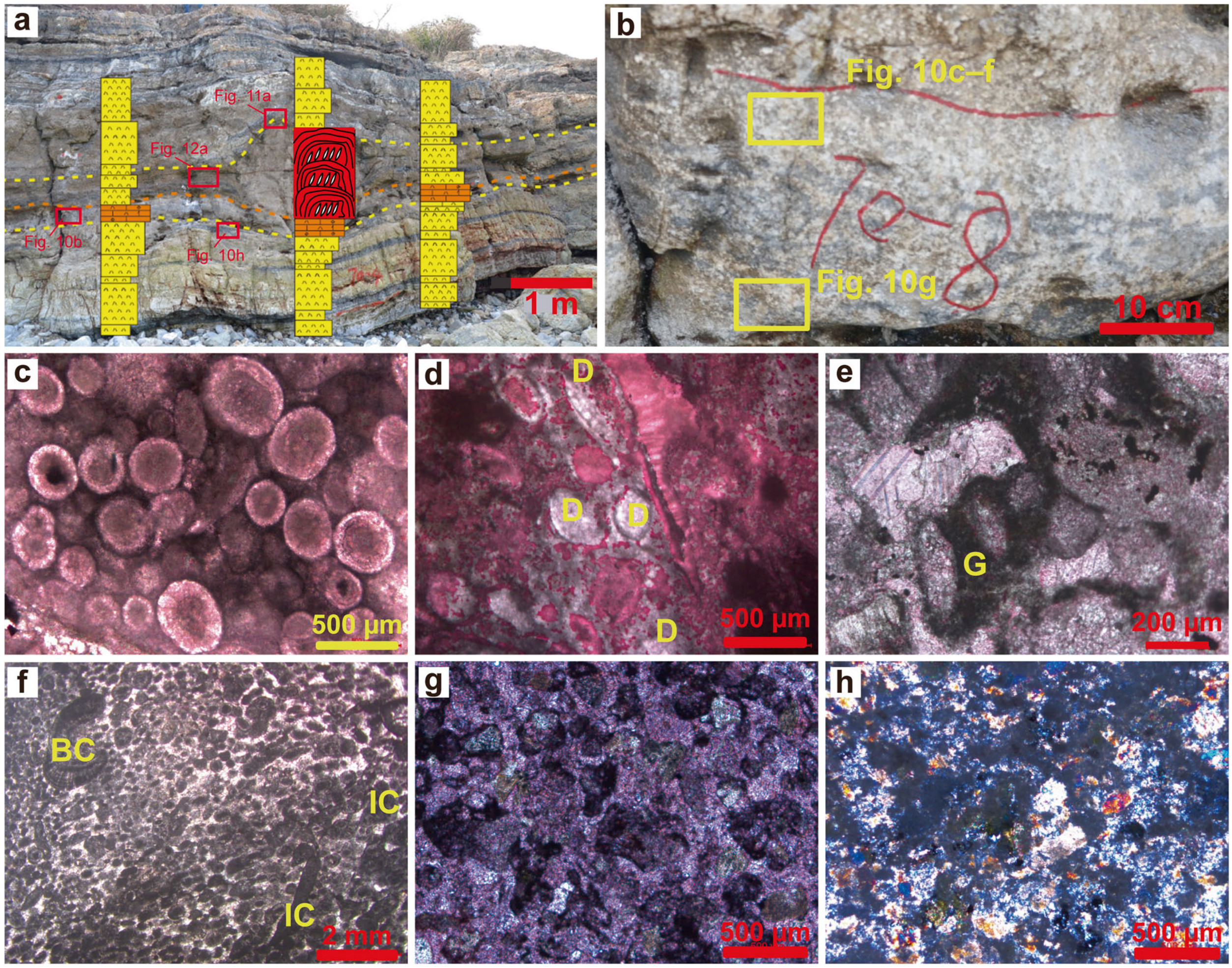

Fig. 10 **a** Field photo showing the reef (outlined) and the overlying and underlying strata in the upper part of assemblage 8 (yellow rectangle in Fig. 4). Below the reef, a grain shoal develop above tuffite. Laminated fine tuffite covers, and prohibits the growth of the reef. Tuffite with coarse fabrics fills the interreef spaces; **b** Meso-photo of the grain shoal. Samples are respectively from the upper (**c**–**f**) and lower part (**g**) of the grain shoal; **c** Oolitic limestone. 5×, plane-polarized light; **d** Dolomitic limestone. Dolomite (D) is unstained. 5×, plane-polarized light; **e** Bioclastic limestone. A gastropod (G) can be seen clearly. 10×, plane-polarized light; **f** Sparry oolitic limestone with intraclasts (IC) and bioclasts (BC). 1.25×, plane-polarized light; **g** Photomicrograph of tuffaceous limestone; some grains are silicate (darker color) not carbonate. Stained thin section, 5×, plane-polarized light; **h** Photomicrograph of limy tuffite. 5×, plane-polarized light

lower part is stromatolite with fan-shaped growth pattern (Fig. 11c). EPMA and EDS analyses show that the laminated fine tuffite is composed of aluminosilicate minerals such as feldspars and abundant pyrite (Fig. 11d).

5.2.2 Tuffite with coarse fabrics

Tuffite with coarse fabrics occurs in the interreef spaces (Figs. 10a and 12a). Photomicrographs of it show many coarse fabrics which are smaller than 2 mm in fine matrix (Fig. 12b, d). These coarse grains contain many aluminosilicate minerals such as analcite (formula: $NaAlSi_2O_6{\cdot}H_2O$), feldspar and pyrite. Analcite is white in color under plane-polarized light (Fig. 12b) and shows complete extinction under cross-polarized light (Fig. 12d). EPMA and EDS analyses (Fig. 12c) show that the minerals showing complete extinction under cross-polarized light are analcites.

5.3 Mixed lithology

Mixed lithology develops at the bottom of the grain bank (Layer 70-8, Fig. 10b) and in Layer 70-7 (Fig. 10a). There are two kinds of mixed lithology: limy tuffite occurs in Layer 70-7 (Fig. 10a, h) and tuffaceous limestone develops at the bottom of the grain bank (Fig. 10b, g).

6 Results

Based on the above description of all types of lithology, from macroscale through mesoscale to microscale, nine microbialite–tuffite assemblages have been recognized in the Shipu section. Their thicknesses increase gradually

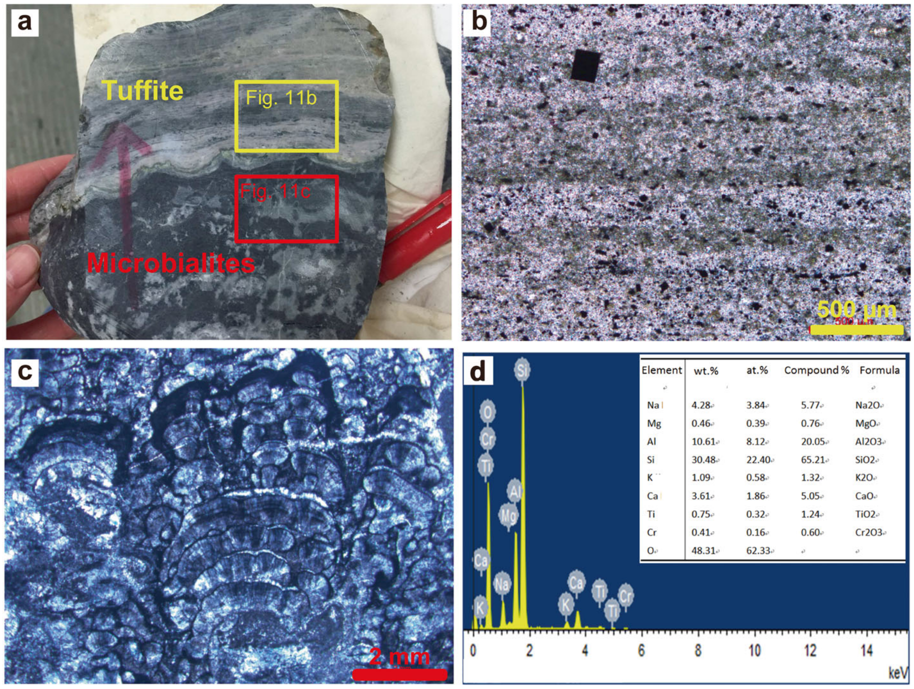

Fig. 11 **a** A hand specimen from the interface between carbonates and tuffite. The upper part is tuffite and the lower part is limestone; **b** Photomicrograph of laminated fine tuffite including pyrite (black color). 5×, plane-polarized light; **c** Photomicrograph of limestone showing fan-shaped growth pattern of stromatolite. 1.25×, plane-polarized light; **d** EPMA and EDS analyses show that the laminated fine tuffite is composed of aluminosilicate minerals such as feldspars

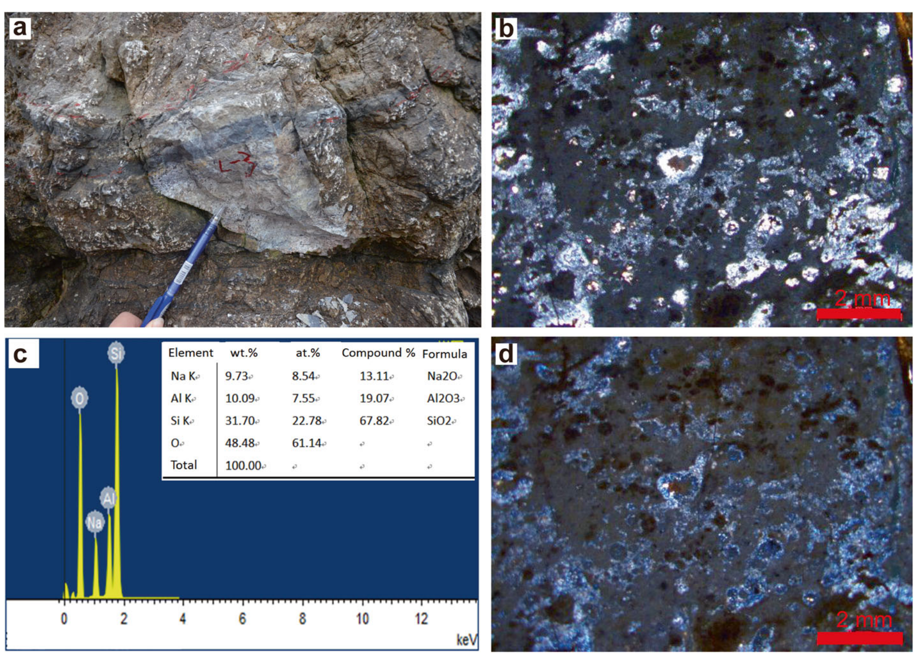

Fig. 12 Tuffite with coarse fabrics in interreef spaces. **a** Meso-photo of tuffite with coarse fabrics; **b**, **d** Photomicrographs of tuffite showing the coarse fabrics including aluminosilicate minerals such as analcite (formula: $NaAlSi_2O_6{\cdot}H_2O$), feldspar and pyrite. Analcite is white under plane-polarized light and shows complete extinction under cross-polarized light. 1.25×; **c** EPMA and EDS analyses show that these minerals are analcites showing complete extinction under cross-polarized light

upwards as volcanic activity decreased. Stromatolites developed in the reef where microbes and serpulids built the framework together. Colonial serpulids are surrounded by microbes which trapped and bound grains to form a reef framework. Below the reefs, a grain bank developed in a high-energy zone near or above fair-weather wave-base. Above the reefs, laminated fine tuffite occurs.

A typical sedimentary cycle, from tuffite through a grain bank to microbial reefs and then tuffite, can be seen clearly in Figs. 3 and Fig. 10a.

7 Discussion

How is it that serpulid-microbial reefs can coexist with tuffite with coarse fabrics, whereas a 5–10-cm-thick laminated fine tuffite layer can stop the growth of reefs? To answer this question, a two-dimensional depositional model has been established which illustrates the palaeoenvironmental evolution for development of the various rock types (Fig. 13).

1) Stage A: Volcanic ash from a distant crater is deposited and forms tuffite (Fig. 3, Layer 70-6, Layer 70-7; Fig. 10h).

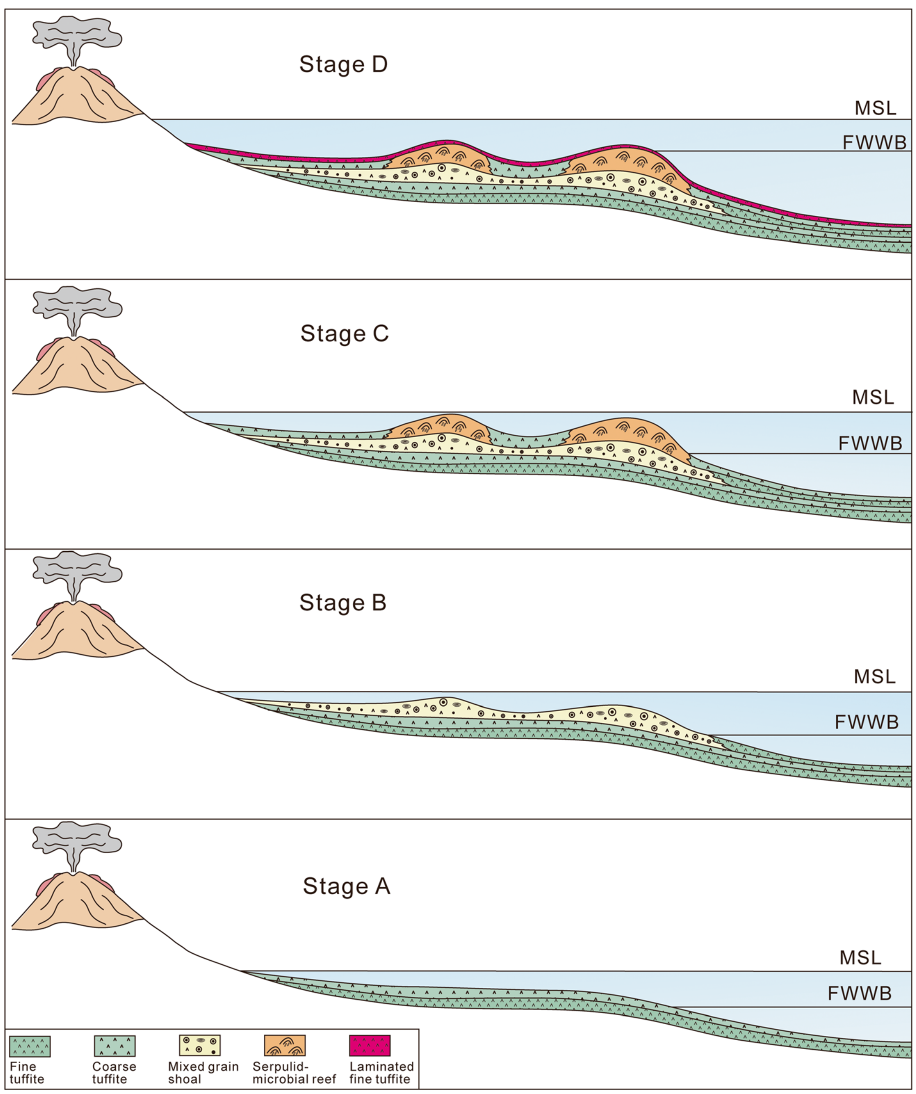

Fig. 13 A two-dimensional depositional model illustrating the palaeoenvironmental evolution for development of the various rock types in the Shipu Group. Stage A: Volcanic ash from a far crater deposit forms tuffite. Stage B: Volcanic ash from a far crater diminishes, and grain shoals develop in a high-energy zone near or above fair-weather wave-base. Stage C: At local high points (grain shoals), serpulid-microbial reefs develop near or above the fair-weather wave-base where waves remove fine volcanic ash and coarser ash is deposited in interreef low spaces due to physical differentiation. Stage D: As the sea level rises, reefs become below FWWB. The waves cannot remove the fine volcanic ash, so the fine volcanic ash inhibits reef growth and is deposited as a laminated fine tuffite layer. MSL: Mean sea level; FWWB: Fair-weather wave-base

2) Stage B: Volcanic ash from a distant crater diminishes, and grain shoals develop in a high-energy zone, near or above FWWB, composed of oolitic limestone and tuffaceous limestone including bioclasts, intraclasts and tuffaceous grains. Some metazoans such as gastropods can be seen in sections which suggests that the water was relatively clean (Fig. 3, Layer 70-8; Fig. 10b–g),
3) Stage C: As the volcanic ash increases, the water quality declines again and many metazoans cannot survive, whereas this environment is very suitable for microbes because macronutrients for microbes are C, N, H, and O, and other nutrients are P, S, K, Mg, Na, Ca, and Fe (Li et al. 2009). Volcanic eruption is important in producing nutrient elements, such as N, P, K, and Fe. It also produces radioactive elements. At local high points (above grain shoals), serpulid-microbial reefs develop near or above FWWB where waves remove fine volcanic ash. Microbes and serpulids build the framework together to resist the waves. However, coarser ash deposits occupy interreef depressions because of physical differentiation.
4) Stage D: As sea level rises, reefs find themselves below FWWB where waves cannot remove fine volcano ash from distant craters. This fine volcano ash inhibits reef growth (too much fine volcanic ash buries the serpulids and microbes) and form deposits of laminated fine tuffite.

8 Conclusions

Based on macroscopic observation of outcrop, microscopic examination of thin sections, EPMA analysis, FESEM imaging analysis and EDS analysis, we can reach the following conclusions:

1) Nine microbialite–tuffite assemblages have been recognized in the section and their thickness increases gradually upwards as volcanism decreases.
2) Serpulid-microbial reefs develop either individually or conjoined with adjacent ones, and consist of stromatolites and serpulid tubes that are commonly recrystallized. Serpulid tubes are calcified and the tube wall is micrite. Tube interiors and intertube areas are filled by sparry calcite. Thus, colonial serpulids are surrounded by microbes to form stromatolites.
3) In the Shipu section, two kinds of accretionary processes generated stromatolites: (i) Fan-shaped stromatolites accreted through the growth of colonies of filamentous microbes (probably cyanobacteria) together with early and pervasive precipitation of carbonate in the EPS sheaths of their filaments. Grains supplied to the stromatolite surface were not trapped and bound in the microbial EPS, but were only deposited between the filament fans. (ii) Flat-shaped stromatolites accreted through the growth of other microbes and grains which were trapped and bound in the uncalcified EPS. Thin micritic crusts separating successive laminae formed during interruption in accretion.
4) Microbes are so well preserved in crystal lattices that the original microstructure of even the cells can be observed clearly by FESEM imaging analysis.
5) In the Shipu section, microbial reefs developed at local high points near or above fair-weather wavebase, where waves removed fine volcanic ash. Interreef deposition was coarse tuffite due to physical differentiation.
6) Volcanic activity could provide rich nutrition for microbes but too much fine volcanic ash inhibited microbial growth. Consequently, moderate supply of volcanic ash favored microbial carbonate development.

Abbreviations

CNPC: China National Petroleum Corporation; EDS: Energy dispersive X-ray spectrometry; EPMA: Electron probe microanalysis; EPS: Extracellular polymeric substances; FESEM: Field emission scanning electron microscopy; FWWB: Fairweather wavebase; MSL: Mean sea level

Acknowledgements

The authors would like to appreciate Hong-Yu Chen, Qian Pan, Si-Cong Luo, Dong-Fang Zhao for sampling and Professor Guo-Hua Zhu for thin-section identification of volcanical rocks. We also sincerely acknowledge Professor Jing-Shan Chen for helpful comments and suggestions on this manuscript and Professor Robert Riding for helping us to revise the manuscript especially language errors. We also gratefully acknowledge the Editor-in-chief, Professor Zeng-Zhao Feng and four anonymous reviewers for their constructive comments and suggestions on this manuscript.

Authors' contributions

XFW, XCT, SNZ and AJS conceived the idea of the study. XFW, XCT, AJS, GH, XW, ZLC, LYP and JZ did the fieldwork and sampling. XFW, XCT, XW and ZLC observed thin sections. XFW, XCT and WC did analytical testing. XFW, XCT, AJS and CL interpreted the results and wrote the paper. XFW and XCT revised the manuscript. All authors read and approved the final manuscript.

Funding

National Major Science and Technology Projects (2016ZX05004–002, 2017ZX05008–005), PetroChina Major Science and Technology Projects (2018A-01, 2019B-0403), and PetroChina Science and Technology Project (2019D-5009-16).

Availability of data and materials

The data analyzed during the current study are available from the corresponding author on reasonable request.

Competing interests

The authors declare that they have no competing interests.

Author details

[1]State Key Laboratory of Oil and Gas Geology and Exploitation, Southwest Petroleum University, Chengdu 610500, Sichuan Province, China. [2]School of Geoscience and Technology, Southwest Petroleum University, Chengdu 610500, Sichuan Province, China. [3]Key Laboratory of Carbonate Reservoirs, China National Petroleum Corporation (CNPC), Hangzhou 310023, Zhejiang

Province, China. [4]PetroChina Hangzhou Research Institute of Geology, Hangzhou 310023, Zhejiang Province, China.

Received: 30 July 2019 Accepted: 23 March 2020
Published online: 20 April 2020

References

Bahniuk, A.M., S. Anjos, A.B. França, N. Matsuda, J. Eiler, J.A. Mckenzie, and C. Vasconcelos. 2015. Development of microbial carbonates in the Lower Cretaceous Codó formation (north-East Brazil): Implications for interpretation of microbialite facies associations and palaeoenvironmental conditions. *Sedimentology* 62 (1): 155–181.

Burne, R.V., and L.S. Moore. 1987. Microbialites: Organosedimentary deposits of benthic microbial communities. *Palaios* 2 (3): 241–254.

Che, Z.Q., X.C. Tan, J.T. Deng, and M.D. Jin. 2019. The characteristics and controlling factors of facies-controlled coastal eogenetic karst: Insights from the fourth member of Neoproterozoic Dengying formation, Central Sichuan Basin, China. *Carbonates and Evaporites* 34 (4): 1771–1783.

Delfino, D.O., M.D. Wanderley, L.H. Silva e Silva, F. Feder, and F.A.S. Lopes. 2012. Sedimentology and temporal distribution of microbial mats from Brejo do Espinho, Rio de Janeiro, Brazil. *Sedimentary Geology* 263: 85–95.

Della Porta, G. 2015. Carbonate build-ups in lacustrine, hydrothermal and fluvial settings: comparing depositional geometry, fabric types and geochemical signature. In *Microbial carbonates in space and time: implications for global exploration and production*, ed. D.W.J. Bosence, K. A. Gibbons, D.P. Le Heron, W.A. Morgan, T. Pritchard, and B.A. Vining, vol. 418, 17–68. London, Special Publications: Geological Society.

Dickson, J.A.D. 1966. Carbonate identification and genesis as revealed by staining. *Journal of Sedimentary Petrology* 36 (2): 491–505.

Hu, G., W.X. Hu, J. Cao, S.P. Yao, Y.X. Li, Y.X. Liu, and X.Y. Wang. 2012b. Zircon U–Pb dating of the Shipu limestone in Zhejiang Province, coastal Southeast China: implications for the Early Cretaceous environment. *Cretaceous Research* 37: 65–75.

Hu, G., W.X. Hu, J. Cao, S.P. Yao, X.M. Xie, Y.X. Li, Y.X. Liu, and X.Y. Wang. 2012a. Deciphering the Early Cretaceous transgression in coastal southeastern China: Constraints based on petrography, paleontology and geochemistry. *Palaeogeography, Palaeoclimatology, Palaeoecology* 317–318: 182–195.

Jahn, B. 1974. Mesozoic thermal events in Southeast China. *Nature* 248 (5448): 480–483.

John, B.M., X.H. Zhou, and J.L. Li. 1990. Formation and tectonic evolution of southeastern China and Taiwan: Isotopic and geochemical constraints. *Tectonophysics* 183: 145–160.

Kershaw, S., S. Crasquin, Y. Li, P.Y. Collin, M.B. Forel, X.N. Mu, A. Baud, Y. Wang, S. Xie, F. Maurer, and L. Guo. 2012. Microbialites and global environmental change across the Permian–Triassic boundary: A synthesis. *Geobiology* 10 (1): 25–47.

Kershaw, S., Y. Li, S. Crasquin-Soleau, Q.L. Feng, X.N. Mu, P.Y. Collin, A. Reynolds, and L. Guo. 2007. Earliest Triassic microbialites in the South China block and other areas: controls on their growth and distribution. *Facies* 53 (3): 409–425.

Lei, C., H. Li, R. Yang, and J. Cheng. 2012. Lacustrine microbial dolomite of the Middle Permian Lucaogou formation in Urümqi, Xinjiang. *Journal of Palaeogeography (Chinese Edition)* 14 (6): 767–775 (in Chinese with English abstract).

Li, F., J.X. Yan, R.V. Burne, Z. Chen, T.J. Algeo, W. Zhang, L. Tian, Y.L. Gan, K. Liu, and S.C. Xie. 2017. Paleo-seawater REE compositions and microbial signatures preserved in laminae of lower Triassic ooids. *Palaeogeography, Palaeoclimatology, Palaeoecology* 486: 96–107.

Li, L., X.C. Tan, W. Zeng, T. Zhou, Y. Yang, H.T. Hong, B. Luo, and L.Z. Bian. 2013. Development and reservoir significance of mud mounds in Sinian Dengying formation, Sichuan Basin. *Petroleum Exploration and Development* 40 (6): 714–721.

Li, M.C., W.B. Yang, et al. 2009. A translated book: Original English language title. In *Brock biology of microorganisms (11th edition)*, ed. M.T. Madigan and J.M. Martinko , 146–147. Beijing: Science Press.2006

Mancini, E.A., W.C. Parcell, W.M. Ahr, V.O. Ramirez, J.C. Llinás, and M. Cameron. 2008. Upper Jurassic updip stratigraphic trap and associated Smackover microbial and nearshore carbonate facies, eastern gulf coastal plain. *AAPG Bulletin* 92 (4): 417–442.

Rezende, M.F., and M.C. Pope. 2015. Importance of depositional texture in pore characterization of subsalt microbialite carbonates, offshore Brazil. In *Microbial carbonates in space and time: implications for global exploration and production*, ed. D.W.J. Bosence, K.A. Gibbons, D.P. Le Heron, W.A. Morgan, T. Pritchard, and B.A. Vining, vol. 418, 193–207. London, Special Publications: Geological Society.

Riding, R. 1991. Classification of microbial carbonates. In *Calcareous algae and Stromatolites*, ed. R. Riding, 21–51. Berlin: Springer-Verlag.

Riding, R. 2000. Microbial carbonates: the geological record of calcified bacterial–algal mats and biofilms. *Sedimentology* 47 (s1): 179–214.

Suarez-Gonzalez, P., M.I. Benito, I.E. Quijada, R. Mas, and S. Campos-Soto. 2019. 'Trapping and binding': a review of the factors controlling the development of fossil agglutinated microbialites and their distribution in space and time. *Earth-Science Reviews* 194: 182–215.

Tang, H., S. Kershaw, H. Liu, X.C. Tan, F. Li, G. Hu, C. Huang, L.C. Wang, C.B. Lian, L. Li, and X.F. Yang. 2017. Permian–Triassic boundary microbialites (PTBMs) in Southwest China: Implications for paleoenvironment reconstruction. *Facies* 63 (1): 2. https://doi.org/10.1007/s10347-016-0482-8.

Tang, X.P., W.H. Huang, H.W. Deng, W.Y. Wang, and N.N. Mu. 2012. Formation mechanisms of the Paleogene lacustrine microbial carbonate rocks in Pingyi Basin, Shandong Province. *Journal of Palaeogeography (Chinese Edition)* 14 (3): 355–364 (in Chinese with English abstract).

Xie, X.M., W.X. Hu, J. Cao, S.P. Yao, L.Z. Bian, and Y.Q. Gao. 2010. Preliminary investigation on depositional environment of black mud in Lower Cretaceous, Zhejiang and Fujian provinces: Micropaleontology and organic geochemical evidences. *Acta Sedimentologica Sinica* 28 (6): 1108–1116 (in Chinese with English abstract).

Xu, B.M. 1991. The revelation of marine Lower Cretaceous series in east area of China and its geological significance. *Donghai Marine Science* 9: 38–45 (in Chinese with English abstract).

Xu, B.M. 1992. A discussion on the age of the Shipu group adjacent to the Shipu town, Xiangshan County, Zhejiang Province. *Experimental Petroleum Geology* 14: 64–67 (in Chinese with English abstract).

Xu, B.M., and S.P. Zheng. 1989. The age and characteristics of sedimentary facies of the "Shipu limestone" in Xiangshan, Zhejiang Province. *Geological Review* 35: 221–230 (in Chinese with English abstract).

Xu, L.M., C.S. Jin, Z.X. Jiang, K. Deng, and D.H. Jiang. 2018. The establishment of marine Early Cretaceous strata in east area of Zhejiang coast and its significance. *Geology of Fujian* 35 (2): 92–100 (in Chinese with English abstract).

Zhang, D.M., T.Z. Duan, Z.M. Zhang, Y. Hao, and W. Yao. 2018. Facies model of lacustrine microbial carbonates: a case study from a oilfield, Santos Basin. *Journal of Northwest University (Natural Science Edition)* 48 (3): 413–422 (in Chinese with English abstract).

Zhou, X.M., T. Sun, W.Z. Shen, L.S. Shu, and Y.L. Niu. 2006. Petrogenesis of Mesozoic granitoids and volcanic rocks in South China: A response to tectonic evolution. *Episodes* 29 (1): 26–33.

Publisher's Note